

DETERMINATION OF FORMING LIMIT CURVES USING 3D DIGITAL IMAGE CORRELATION AND IN-SITU OBSERVATION

Ala Hijazi^{*}, Nikhil Yardi[†] and Vis Madhavan[‡]
Department of Industrial and Manufacturing Engineering
Wichita State University
1845 Fairmount, Wichita, KS 67260-0035

ABSTRACT

The use of finite element analysis in process design of sheet metal forming has become a standard practice. Forming limit curves are used in finite element simulations of sheet metal forming to check for possible failure of the sheet. Forming limit curves are typically determined using the limiting dome height test and the strain circle technique. With the development of the three-dimensional digital image correlation technique, it has become possible to determine the forming limit curves with a higher accuracy and less effort typically by comparing images of the test specimens at the end and at the beginning of the test. A limiting dome height tool has been designed such that it permits in-situ observation of the part while it is being formed. Combining in-situ observation with three-dimensional digital image correlation, it is possible to monitor the evolution of strain throughout the sheet from the beginning of the forming to the failure of the sheet. This eliminates the need for an abort criterion since limiting strains can be obtained by considering the deformation stage just before the onset of localized necking. Using this technique, forming limit curves for different aluminum alloys have been determined. The effects of anisotropy and lubrication on limiting strains have also been investigated.

KEY WORDS: Formability, Testing/Evaluation, Optical Testing

1. INTRODUCTION

Sheet metal forming is a common manufacturing process used to plastically deform flat sheets into desired 3D shapes. The Keeler-Goodwin diagram or Forming Limit Diagram (FLD) is a convenient and often used tool for the evaluation of sheet metal forming processes. A Forming Limit Curve (FLC) is a representation of the ductility of a material under different combinations of major and minor strains. The FLC of a given material defines the boundary between strain combinations that produce failure and those that are permissible in forming operations.

* Research Scientist

† Graduate Student

‡ Associate Professor

The test typically used to determine the FLC is the Limiting Dome Height (LDH) test, in which a hemispherical punch is used to deform the sheet until failure occurs. Figure 1 shows a schematic diagram of the LDH test. By testing specimens of different widths, different combinations of major and minor strains can be obtained in the sheet prior to fracture. These combinations of major and minor strains (at failure) define the FLC of the corresponding material.

In the research described herein a modified LDH test tool that enables in-situ observation of the specimen has been developed and 3D Digital Image Correlation (DIC) of recorded images is used to obtain the strains. A procedure for determining the FLC using in-situ observation has been introduced and applied to determine the FLCs for two sheet thicknesses of three different aluminum alloys (1), however, only representative data is presented herein. The effects of anisotropy and lubrication on limiting strains have also been investigated.

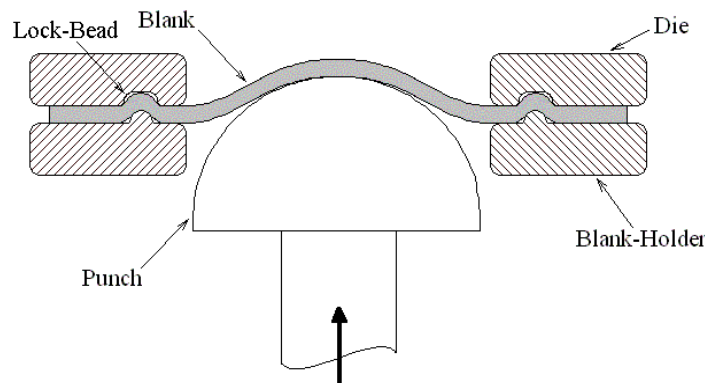


Figure 1: Schematic (sectional view) of the LDH tester.

2. BACKGROUND

According to the ISO-12004 standard (2), any set of tooling employing a holding force and deformation force may be used to develop the limiting strain condition. A number of different tests have been used for measuring the formability of materials. The Erichsen test (3) consists of a flat polished blank-holder holding the sheet on a die with a circular opening of 27mm. The blank is formed using a 20mm diameter spherical punch and the test is stopped at failure of the blank. The failure height is termed as the Erichsen number. The Olson test (3) is a US equivalent of the Erichsen test where a 22mm (7/8 inch) punch is used with a die opening of 25mm (1 inch). The Olson test has been found to have poor repeatability where the scatter in the data is more than that attributable to the variation in material properties. The poor repeatability has been attributed to the small size of the punch and the absence of lock-bead on the blank-holder to restrict the material draw-in leading to uneven draw-in (3). Hecker developed a new test rig with a lock-bead to hold the blank, a 101.6mm (4 inch) diameter punch and a die opening of 105.7mm (4.16 inch) (3). The Hecker test is more commonly known as the LDH test. The LDH test is the most commonly used test for determining FLCs.

Over the past three decades, the strain circles technique, developed by Keeler (4) in 1968, has been commonly used to measure plastic strains developed during sheet metal forming. A pattern of fine circles is created on the blank using electro-chemical etching, or more recently using

enamel or vinyl-based ink. Keeler proposed different patterns and strain circle sizes depending on the type and amount of deformation observed during forming. As the sheet deforms, the circles deform into ellipses. The major and minor principal strains are obtained by measuring the major and minor axes of the ellipse, assuming monotonic deformation of the sheet. A stencil is usually used to measure the major and minor diameters of the ellipse. However, the use of the strain circles technique is tedious and leads to errors due to variation in initial diameter of the circles (up to 2% is acceptable according to ISO-12004 standard), human error in comparing with templates and curvature of the sheet.

With recent developments in Charged Coupled Device (CCD) cameras and use of stereographic photography to obtain a 3D image of the part under observation, it has become possible to map the strain distribution on surfaces of deformed sheets, using DIC, without the need for applying a uniform pattern (grid pattern) to the sheet before forming. The DIC method is based on the principle that the light intensity variation within regions of the image, called facets or subsets, in the un-deformed state can be correlated with the intensity distribution in the deformed state to determine the new location of the subset (5). Three-dimensional DIC is based on the principle of photogrammetry where two CCD cameras (or more), in stereoscopic configuration, are used to observe the part under consideration. With a known position of the two cameras (determined using prior calibration with a standard target) and two homologous image points, the 3D coordinates of the surface points can be determined (6). As the part undergoes deformation, displacement vectors and therefore local strain values can be obtained. The sensitivity of displacement fields obtained using 3D DIC is typically 1/30,000 of the field of view (7).

Hotz and Hanggi (8) demonstrated the use of 3D DIC for determining FLCs using the LDH test, where a random spray paint pattern applied to the sheet prior to deformation and images before and after the test were used for the image correlation. Vacher et al. (9) used 2D image correlation to determine the FLC for SOLDUR 340 steel alloy using a test similar to the Swift cup test. In both cases, the final deformed images were directly compared with the initial un-deformed images, without in-situ observation.

Use of only the final and initial images to determine the limiting strains makes it important to stop the test just before failure. This is done by first determining the limiting dome height (i.e., the height at which failure occurs) for a given material and blank geometry, then using this height as an abort criterion (i.e., the test will be stopped before reaching this height) (8). However, the failure height varies due to non-uniformity of the specimens (in terms of material properties, sheet thickness etc.) which typically leads to conservative estimates of the limiting strains.

In this study, in-situ optical observation is combined with 3D DIC to obtain the strain history in the sheet (i.e., through the forming process). By using the data immediately prior to the onset of localized necking (or fracture, if desired), the need for an abort criterion is eliminated.

3. EXPERIMENTAL PROCEDURE

The LDH test was used to form the sheet until failure in order to determine the FLC. A modified LDH test tool which permits observation of the sheet during forming was used for the

experiments. The tool was designed such that a single actuator of a universal testing machine (UTM) can be used to apply the required blank holding force and then to apply the force needed to form the sheet. Strain measurements were made using the ARAMIS (10) 3D DIC system.

3.1. Tool Design

The North America Deep Drawing Research Group (NADDRG) has established guidelines for the LDH test (11). According to the NADDRG specifications, the punch should be a sphere of radius $50.8 \pm 0.03 \text{ mm}$ (2 ± 0.0012 inch), the punch speed should be $250 \pm 25 \text{ mm/minute}$ (9.84 ± 1 inch/minute), the Blank Holding Force (BHF) should be 200-511KN (45-115 kips) and the draw-in of the blank during the test should not exceed 0.25mm (0.01 inch). Due to concerns about the probability of failure of the sheet at the lock-bead, the lock-bead design was investigated for Al 2524-T3 as it is the least ductile material among the materials under consideration. A full width specimen of Al 2524-T3 was tested using an existing tool manufactured according to the NADDRG recommended geometry (11). The specimen fractured at the lock-bead during the test, as seen in the Figure 2. To avoid this, the design was modified by reducing the height of the lock-bead from 4.6mm to 3.56mm.



Figure 2: Tearing of Al2524-T3 specimen at lock-bead during the test.

A 3D DIC system, ARAMIS (10), was used for measuring the strains. Two CCD cameras in stereoscopic configuration were used to capture the forming process. In order to observe the blank while forming is in progress, the height of the die was increased and two cuts were made in the sides of the die to permit visibility of the blank. An exploded view of the tool components is shown in Figure 3. A mirror oriented at 45° to the plane of the blank was placed within the die in order to view the blank indirectly, as shown schematically in Figure 3. The tool was designed to be used on a standard UTM machine that has a single actuator. Hence, a sleeve that is used to apply the required BHF uniformly was incorporated in the design. The sleeve, shown in Figure 3, is a hollow tube which fits over the punch, and transmits the load from the base of the punch to the blank-holder.

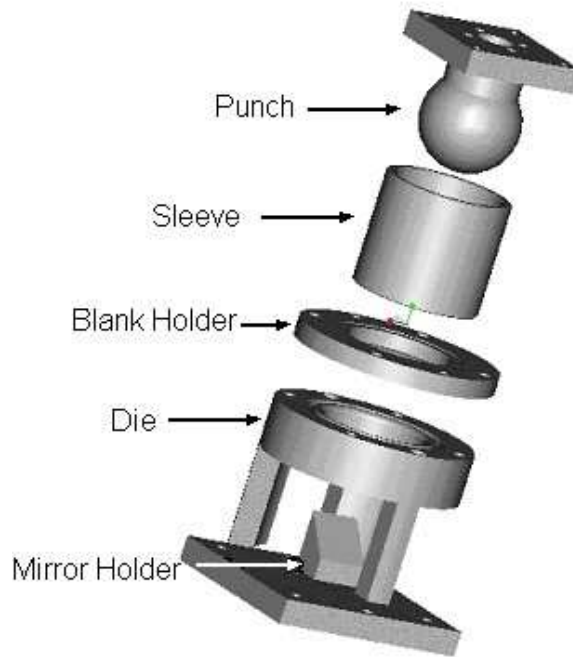


Figure 3: Exploded view of the LDH tool components.

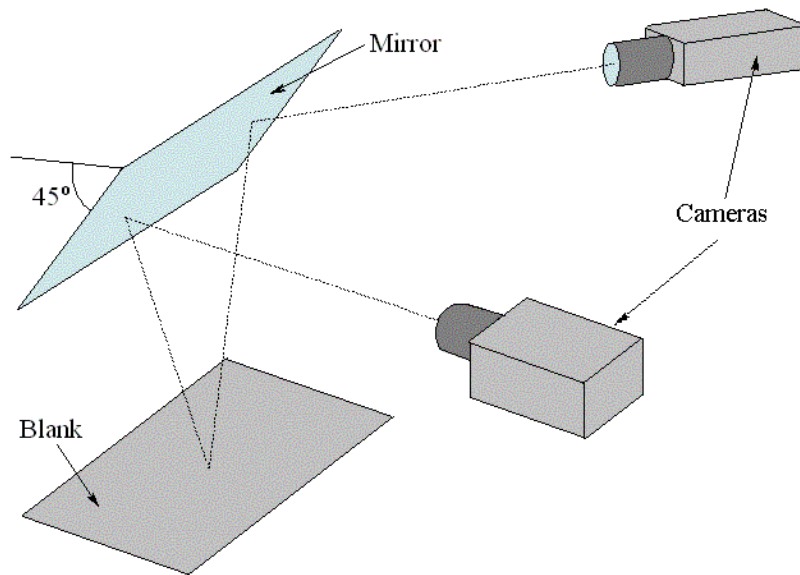


Figure 4: Schematic of the arrangement of the cameras and the mirror.

3.2.Design of Blanks

The right hand side of the FLC is obtained by subjecting the blank to biaxial stretching. This is achieved by holding the specimen, while being formed, around the entire circumference by the

lock-bead. Such a specimen will henceforth be referred to as a full width specimen. The left hand side of the FLC is obtained by testing reduced width specimens of various widths. NADDRG recommends a rectangular shaped blank for reduced width specimens (11). However, rectangular specimens of the aluminum alloys tested here were found to fail at the bend radius of the lock-bead due to stress concentration, as can be in Figure 5. Upon experimenting with different designs, it was found that circular cutouts proved to be the most appropriate. Figure 6 shows specimens of different widths used in the tests.

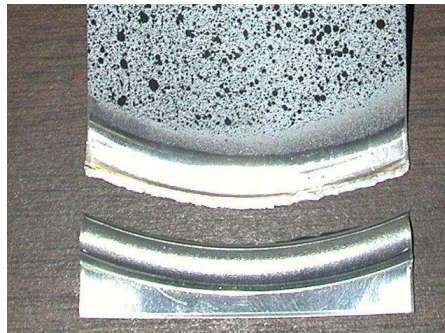


Figure 5: Fracture of reduced-width rectangular specimen during the test.

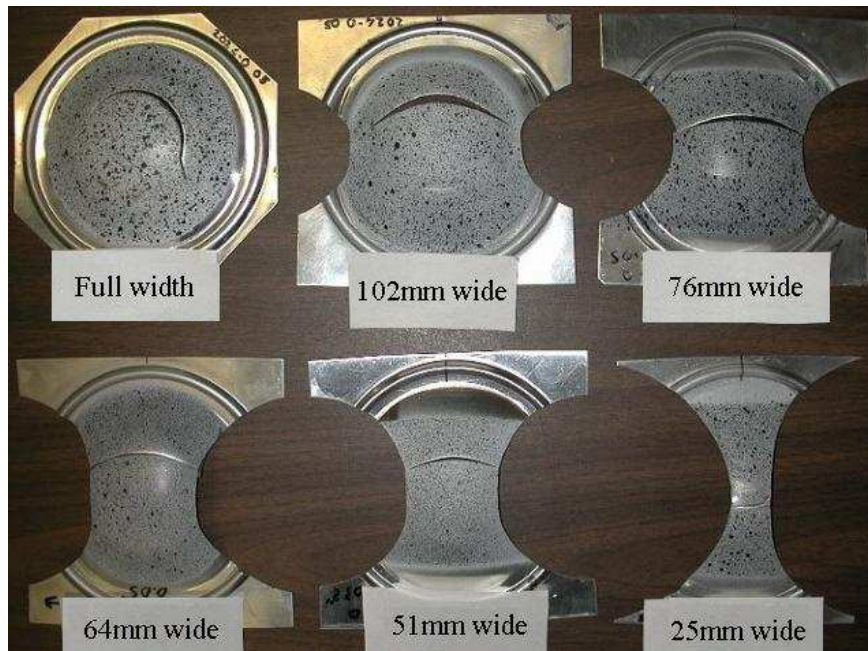


Figure 6: Specimens of different widths.

3.3. Test Matrix

Forming limit curves were determined for two sheet thicknesses of Al 2024-O alloy. The data points needed to define the right-hand-side of the FLC are obtained by testing full width specimens under different friction conditions, where the less the friction the more the point is moved to the right. Full width specimens were tested in both the dry and lubricated conditions using two different lubricants, wax and Boe-Lube. The data points on the left-hand-side of the

FLC are obtained by testing specimens of various widths, where the less the width the more the point is moved to the left (i.e., closer to the simple tension line). The reduced width specimens were tested in 0°, 45° and 90° grain orientations in order to characterize the effect of grain orientation on the left-hand-side of FLCs. Also, reduced width specimens were tested in the dry and the lubricated conditions to investigate the effect of lubrication on the left-hand-side of the FLC.

3.4. Experimental setup

The tool was first assembled away from the testing machine then it was mounted on a 98KN UTM machine using 1.5 inch diameter studs and spiral washers. Any misalignment between the die and the punch can cause asymmetric deformation, thus special care was given to aligning the punch and the die properly. To keep the cameras stationary, the die assembly was mounted on the load cell (which is attached to the stationary crosshead) and the punch assembly was mounted on the actuator. Figure 7 shows the LDH tool mounted on the testing machine.

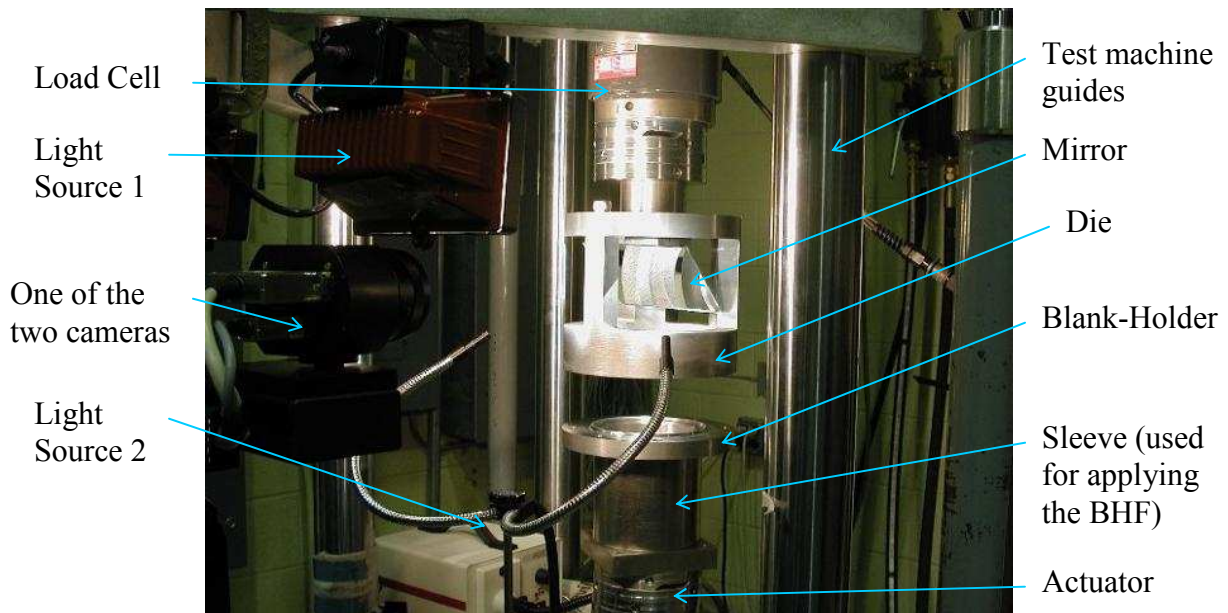


Figure 7: The test setup (the punch is not seen in this picture since it is covered by the sleeve).

The two CCD video cameras, mounted in a stereoscopic configuration, view the specimen indirectly through the mirror. An area of approximately 100×75mm of the blank is to be monitored during the tests. Therefore, a similar size calibration object (100mm×80mm) was used and a standard calibration procedure was carried out (10). Lenses with 50mm focal-length were used to obtain the required magnification. The distance between the camera and the blank when viewed through the mirror was 63.5cm and the angle between the two cameras was maintained at 32.8°. Each of the two CCD cameras has a resolution of 1280×1024 pixels and can record up to 20 frames per second. Multiple light sources were used to illuminate the blank from multiple angles to assure consistent light intensity throughout the forming process.

According to NADDRG, the draw-in of the material over the lock-bead should be less than 0.25mm and the recommended BHF is 200-511KN (11). However, at loads much lower than the

recommended BHF, it was observed that there was practically no draw-in of the material. Furthermore, it was observed that a BHF of 200KN causes the 1.25mm thick Al 2524-T3 full width specimens to fail at the lock-bead. A BHF of 133KN was found to prevent draw-in and at the same time it does not cause fracture of the specimen at the lock-bead. Hence, a BHF of 133KN was used for all the full width specimens. For the reduced width specimens, the holding force was calculated by linear interpolation based on the circumference of the specimen held in the lock-bead.

3.5. Test Procedure

Each of the specimens is cleaned with acetone prior to the test. It is then painted on the side away from the punch. Paint is applied only to the center area of the specimen (i.e., the area that is being observed by the cameras). Spray paint with matt finish is used to minimize specular reflections. A uniform thin layer of white paint is applied. On top of it, an arbitrary pattern of small black dots is created by spraying black paint from afar. Symmetry lines are marked on the reduced width specimens and used to align the blank with respect to the die. After placing the blank between the die and the blank holder, the sleeve is used to apply the required BHF. Four bolts are then used to maintain the BHF and the sleeve is removed. The punch motion is then initiated at a speed of 25 cm/min to form the sheet. Image acquisition at 10 fps is initiated simultaneously with the beginning of the punch motion. The test is stopped after fracture of the specimen.

3.6. Computation of Limiting Strains

The average number of images captured for typical test was about 120 images (60 from each of the two cameras). This large number of frames is needed in order to be able to detect the onset of localized necking. An image just before necking occurs is selected as the last image to be analyzed. A facet size of 31 pixels and step size of 29 pixels was used to perform the DIC. A facet size of 31 pixels corresponds approximately to 2.5mm on the surface of the blank, which is close to the size of the circular grid used in the conventional strain circle technique. A step size of 29 pixels indicates that the distance between the centers of adjacent facets is 29 pixels. The overlapping of adjacent facets helps in pattern matching for the two images obtained from different angles. The "step" method (i.e., the total deformation is obtained by comparing successive images on a step-by-step basis) was used for the analyses such that strains are obtained at all stages of the forming process. The "multi-facet" option was used to analyze the images since it yields a higher accuracy (10). Figure 8 shows the fringes of major strain obtained during different stages of the deformation process up to the last frame from which the limiting strain value is determined.

Major and minor strain values for each facet for the final stage of deformation are exported and plotted using MS-Excel to generate the FLD of a particular test, as shown in Figure 9(a). The point marked with an x in Figure 9(b) is obtained by averaging the 10 points with the highest major strains. This is taken to be the limiting strain. A set of such limiting strain points obtained in a similar manner from full width specimens with different friction conditions and reduced width specimens of various widths would define the FLC for a given material.

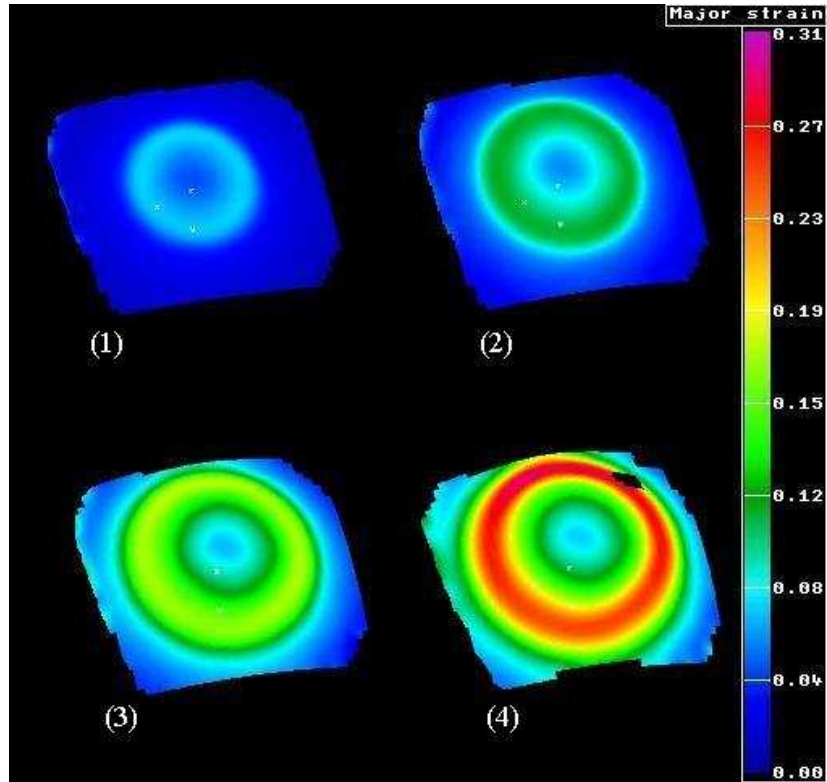


Figure 8: Major strain distribution during different stages of the forming process.

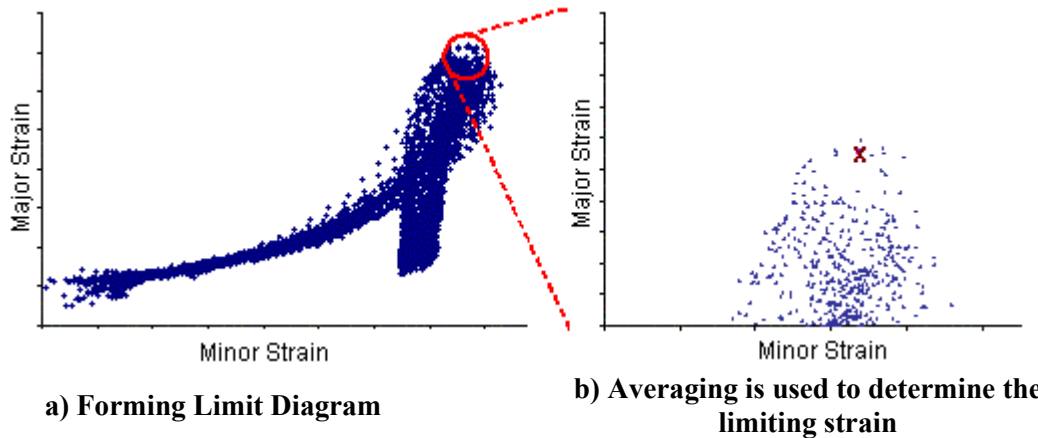


Figure 9: Determination of the limiting strain values used to obtain each point of the FLC.

4. RESULTS AND DISCUSSION

Forming limit curves were determined using the procedure described above for 0.81mm and 1.25mm thick Al 2024-O sheets. Figure 10 shows the FLC for 1.25mm thick Al 2024-O sheet along with the strain data points from each of the different specimens that were used to generate it.

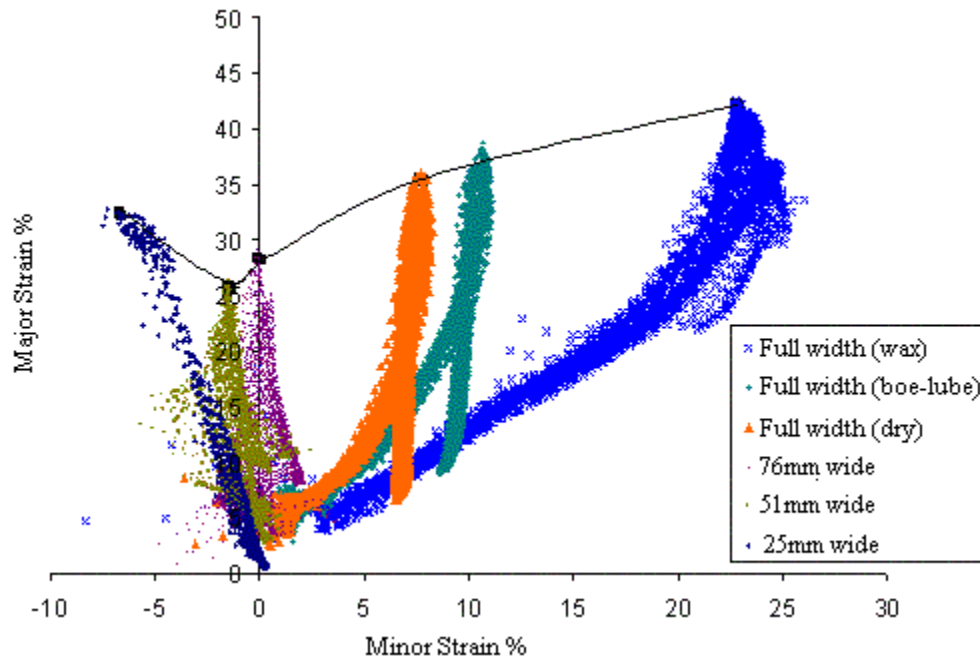


Figure 10: FLC for 1.25mm thick Al 2024-O and the strain data used to generate it.

It should be noted that with the in-situ observation technique, the strains are calculated while the specimen is still loaded (i.e., the punch is still in contact with the specimen such that the elastic strains in the sheet are not released). In the conventional method the specimen is removed from the tool and allowed to spring-back before measuring strains. The strain measured for a loaded blank will be higher than the strain measured after releasing the load. This, and the fact that the test is not aborted, result in FLCs that are less conservative (more realistic) than those obtained using the conventional method.

4.1.Effect of material thickness

Figure 11 shows the FLCs for 1.25mm and 0.81mm thick Al 2024-O sheet. It can be seen that limiting strains increase with increasing sheet thickness. Though not shown here, the other materials tested also showed a similar trend. This is similar to the finding by Gosh (12) which he attributes to the more uniform distribution of the strain as the sheet thickness increases.

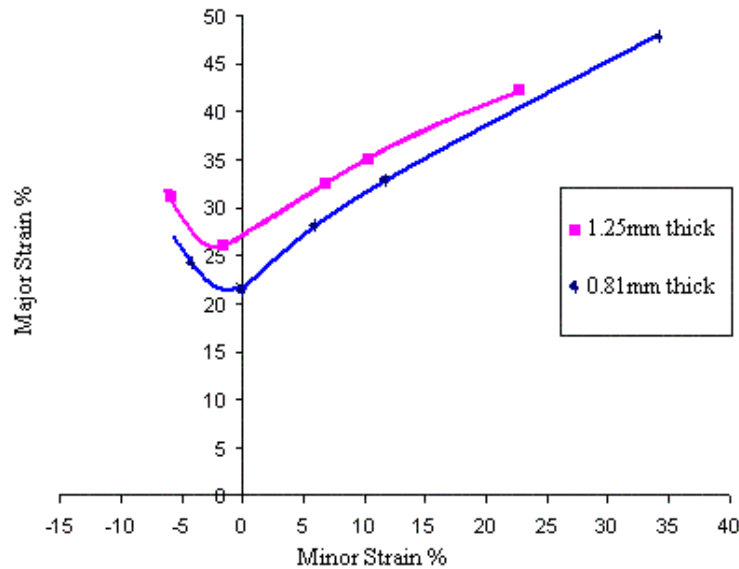


Figure 11: Effect of sheet thickness on limiting strains (Al 2024-O).

4.2. Effect of lubrication

To investigate the effect of friction on formability, specimens were tested under different friction conditions. Full width specimens of Al 2024-O were tested in the dry condition as well as using two different lubricants, namely Boe-Lube and Wax. Figure 12 shows three specimens tested under different friction conditions where the difference in failure height can be observed visually. Lubrication increases both the major and minor strains with the increase in minor strain being more significant, as can be seen in Figure 10.

Reduced width Al 2024-O specimens were also tested in the dry and lubricated conditions. In this case, the effect of lubrication on formability was found to be dependent on the specimen width. Figure 13 shows the effect of lubrication on limiting strain for 1.25mm thick 2024-O sheet. It can be seen from the figure that lubrication does not affect the limiting strain for the 51mm and 64mm wide specimens, whereas it causes a noticeable increase in the major and minor strains for the 25mm wide specimen. In general, it can be said that lubrication increases formability under biaxial stretching (i.e., the right-hand-side of the FLC) and uniaxial stretching (i.e., the left-hand-side of the FLC), while it does not have a clear effect in the plane strain region.



Figure 12: Effect of friction on formability of full width specimens.

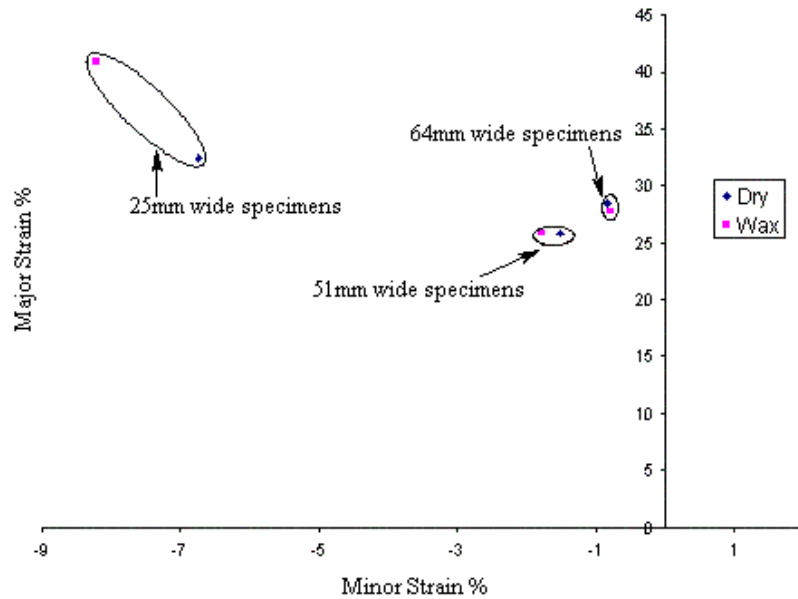


Figure 13: Effect of friction on formability of reduced width specimens.

4.3. Effect of grain orientation

Rees (13) investigated the effect of grain orientation on the formability of zinc clad CR steel sheets. He reported that grain orientation has very little effect in the zero minor strain region while it is influential in the negative minor strain region of the FLD with the 45° orientation specimens having the highest limiting strain. Similar results were observed in our experiments, where the limiting strain was nearly the same in the plane strain region for all grain orientations, whereas in the negative minor strain region the effect of sheet orientation was evident. Figure 14 shows the limiting strain values for reduced width 1.25mm thick Al 2024-O specimens in different grain orientations. The 45° orientation had the highest limiting strain for the points in the negative minor strain region.

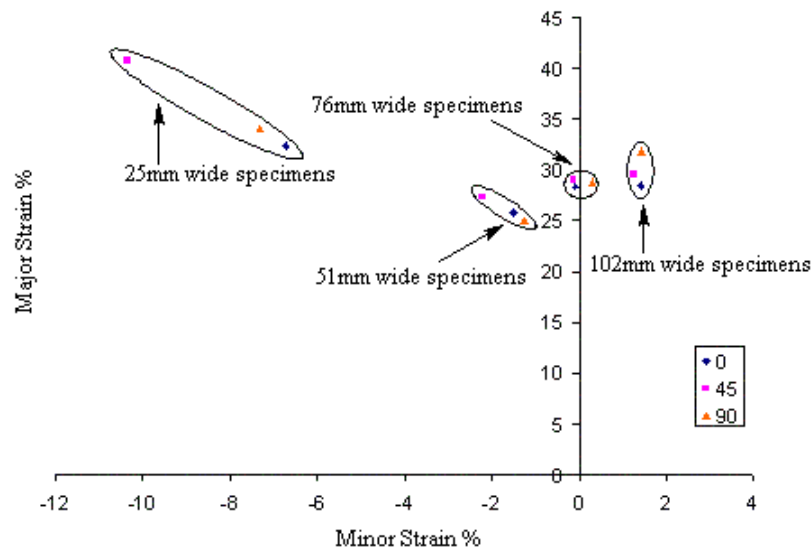


Figure 14: Effect of grain orientation on limiting strain.

5. CONCLUSIONS

The LDH test and in-situ 3D DIC were used to determine the FLCs for 1.25mm and 0.81mm thick aluminum 2024-O sheets. A modified LDH test tool that enables in-situ strain measurements was developed and a new approach to determine FLCs using in-situ strain measurement has been introduced. With in-situ strain measurements the need for an abort criterion is eliminated and the limiting strains can be determined with better accuracy. In addition, the evolution of strain can be tracked throughout the forming process. Using the inverse analysis method, the strain history coupled with finite element simulations can be used to determine the friction coefficient for the stretching mode of deformation. The effects of sheet thickness, anisotropy and lubrication on limiting strains were investigated. The limiting strain values were found to increase with increasing sheet thickness. Anisotropy has a noticeable effect on limiting strain in the left-hand-side of the FLC, with higher formability for the 45° grain orientation. Lubrication increases formability in both the left and right-hand-sides of the FLC while it does not have much effect in the plane strain region.

ACKNOWLEDGEMENT

This work was sponsored by Cessna Aircraft Company and their support is greatly appreciated.

REFERENCES

1. N. Yardi, "Generation of Forming Limit Curves and Friction Coefficient Data for Aluminum Alloys", MS Thesis, Wichita State University, 2003.
2. ISO 12004:1997(E), "Metallic Materials – Guidelines for the Determination of Forming Limit Diagrams", ISO, 1997.
3. S. Hecker, Metals Engineering Quarterly, 14, (4), 30 (1974).
4. S. Keeler, "Circular Grid System - A Valuable Aid for Evaluating Sheet-metal Formability", Society of Automobile Engineers, TP # 680092, 1968.
5. M. Sutton, T. Chae, J. Turner and H. Bruck, ASTM Special Technical Publication, (1094), 1991, pp. 109-132.
6. J. Helm, M. Sutton and S. McNeill, Proceedings of SPIE - The International Society for Optical Engineering, 2350, 1994, pp. 32-45.
7. T. Schmidt, J. Tyson and K. Galanulis, "Advanced Photogrammetry for Robust Deformation and Strain Measurement", Proceedings of SEM 2002 Annual Conference, 2002.
8. W. Hotz and P. Hänggi, "Determination of Forming Limit Diagrams Using ARAMIS", Technical report, GOM, Germany, 2001.
9. P. Vacher, R. Hadder and R. Arrieux, Annals of the CIRP, 48, (1), 227 (1999).
10. ARAMIS User Manual, GOM, Germany, 2000.
11. LDH Test Geometry Benchmark Problem, Proceeding of NUMISHEET 96, 1996, pp. 428-444.
12. A. Gosh in D. Koistinen and N. Wang, eds., Mechanism of Sheet Metal Forming: Material Behavior and Deformation Analysis, Plenum Press, New York, 1978, pp. 287-312.
13. D. Rees, Journal of Material Processing Technology, 118, 1, (2001).